Bioorganic & Medicinal Chemistry Letters 24 (2014) 5107–5110

Contents lists available at ScienceDirect

Bioorganic & Medicinal Chemistry Letters

journal homepage: www.elsevier.com/locate/bmcl

Discovery of a nanomolar inhibitor of lung adenocarcinoma in vitro

Jadd R. Shelton [a], Jan Balzarini [b], Matt A. Peterson [a,*]

[a] Department of Chemistry and Biochemistry, Brigham Young University, Provo, UT 84602, United States
[b] Rega Institute for Medical Research, KU Leuven, B-3000 Leuven, Belgium

ARTICLE INFO

Article history:
Received 1 July 2014
Revised 18 August 2014
Accepted 20 August 2014
Available online 3 September 2014

Keywords:
Purine nucleosides
Bio-active adenosine derivatives
Antiproliferative nucleosides
Lung adenocarcinoma

ABSTRACT

Efficient methods for the preparation of 5′-substituted 5′-amino-5′-deoxy-N^6-ureidoadenosine derivatives are described. Compounds were screened for antiproliferative activity against a panel of murine and human cell lines (L1210, CEM, and HeLa) and/or against the NCI-60. The most potent derivative inhibited the lung adenocarcinoma cell line NCI-H522 at low nanomolar concentrations (GI_{50} = 9.7 nM).

Nucleoside derivatives continue to attract significant interest as templates for the development of anticancer[1] or antiviral[2] chemotherapies. Over the past several decades, numerous derivatives have been made, and a number of such analogs have proven useful as treatments for cancer or viral diseases. As part of research directed toward the discovery of nucleoside-based HIV-integrase inhibitors, we discovered that N^6,5′-bis-ureidoadenosine derivatives **1** and **2** exhibited promising antiproliferative activities against a number of cancer cell lines in vitro (Fig. 1).[3] Structure activity relationship studies (SAR) revealed that the 3′-C methylcarbonyl group was not necessary for activity, and compound **3a** (R^1 = *tert*-butyldimethylsilyl (TBS)) exhibited similar activity to **1** and **2** in the NCI-60.[4] SAR at the 2′,3′ positions showed that acid-stable protecting groups such as triisopropylsilyl (TIPS) and *tert*-butyldiphenylsilyl (TBDPS) were not well tolerated (IC_{50} values for **3c** and **3d** were approximately two orders of magnitude >**3a** for the panel of cell lines evaluated); in contrast acid-labile protecting groups such as triethylsilyl (TES) and certain acyl protecting groups were well tolerated (**3b** was equipotent to **3a** while **4d–f** were only three to five fold less active).[5] SAR at the N^6 position showed that variation of the N^6-ureido substituent (R^3) had very little impact (IC_{50} values for **5a–g** were similar to **3a**), whereas derivatives lacking an N^6-ureido group were essentially inactive.[6]

Preliminary mechanistic studies[6] had supported the conclusion that compounds **1–5** exert their antiproliferative effects via inhibition of bone morphogenetic protein receptor 1b (BMPR1b). BMPR1b is a transmembrane protein receptor that plays a key role in regulating expression of inhibitor of differentiation gene 1 (Id1).

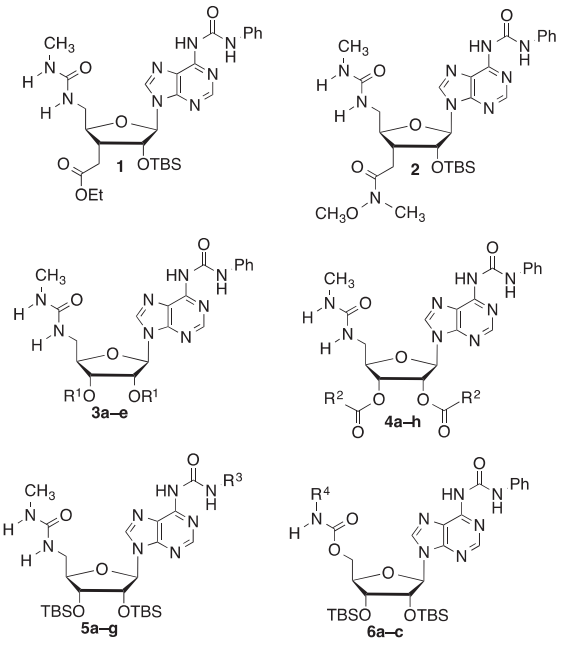

R^1 = **a**-t-BuMe$_2$Si, **b**-Et$_3$Si , **c**-t-BuPh$_2$Si, **d**-(iPr)$_3$Si, **e**-H; R^2 = **a**-CH_3, **b**-*n*-C_3H_7, **c**-$(CH_3)_2CH$, **d**-$C(CH_3)_3$, **e**-*n*-C_5H_{11}, **f**-*n*-C_7H_{15}, **g**-*n*-C_9H_{19}, **h**-*n*-$C_{15}H_{31}$; R^3 = **a**-4-Cl-C_6H_4, **b**-4-I-C_6H_4, **c**-3-I-C_6H_4, **d**-4-CH_3O-C_6H_4, **e**-$C_6H_5CH_2$, **f**-*c*-C_6H_{11}, **g**-*n*-C_3H_7; R^4 = **a**-C_6H_5; **b**-*n*-C_3H_7; **c**-$CH_2CO_2CH_3$

Figure 1.

* Corresponding author.

http://dx.doi.org/10.1016/j.bmcl.2014.08.044
0960-894X/

BMPR1b is a serine/threonine protein kinase with a cytosolic ATP-binding domain that phosphorylates SMADs 1/5/8 as part of the signaling cascade that regulates expression of Id1. Competitive inhibition of binding assays revealed that desilylated derivative **3e** inhibits binding of the immobilized ATP-binding site ligand to BMPR1b (K_d = 11.7 ± 0.5 μM).[6] In contrast, **3a** did not inhibit binding in this assay, thus suggesting that **3a** may act as a prodrug form of the biologically active derivative **3e**.[5] Docking of **3e** in the active site of BMPR1b showed that the lowest energy pose binds with the 5′-terminus embedded deep inside the ATP binding pocket, with the remaining portions of the molecule extending toward the solvent accessible surface (Fig. 2). In this pose, the N^6-phenylureido group is the functionality in closest proximity to the solvent surface, while the 5′-ureido group is proximal to the catalytic triad (K231, E244, D350) and gatekeeper residues (L277). Because of the close proximity of the 5′-position to these key residues, we reasoned that SAR at the 5′ position might conceivably yield ligands with tighter binding. Here, we report the synthesis and biological evaluation of a number of derivatives of **3a** varying at the 5′-position, one of which exhibited potent activity against lung adenocarcinoma cell line NCI-H522 in vitro (IC_{50} = 9.7 nM).

Our initial efforts focused on evaluating the effect of simple replacement of the 5′-NH with a 5′-O-carbamyl group (derivatives **6a–c**, Fig. 1). Consistent with our earlier findings, IC_{50} values for **6a–c** were approximately two orders of magnitude >**3a**, thus confirming the critical nature of the 5′-NH group for biological activity (Table 1).[6] Additional analogs varying at the 5′-position were prepared as outlined (Schemes 1 and 2). Pivotal intermediates in these syntheses were compounds **8** and **12**. Compound **8** was prepared via hydrogenolysis of **7** which could easily be prepared from 5′-chloro-5′-deoxyadenosine via a three-step two-pot reaction sequence previously reported from our laboratory.[4] Treatment of **8** with either phenylisocyanate or the appropriate *N*-alkyl *p*-nitrophenylcarbamate gave compounds **9a–c** in acceptable yields (30–55%). Alternatively, **8** could be acylated with chloroacetylisocyanate to give **10a** (64%) or sulfonylated with methanesulfonyl chloride or *p*-toluenesufonyl chloride to give **11a** and **11b** in 79% and 59% yields, respectively. Compound **10a** was converted to **10b** using classical Finkelstein[7] conditions and gave the desired iodo product in 81% yield. Treatment of **8** via a modified Kočovský carbamylation[8] method gave compound **12** (81%). Treatment of **12** with trifluoroacetyl chloride or monofluoroacetyl chloride gave **13a** and **13b** in 66% and 51% yields, respectively. Compound **12** could also be treated sequentially with the modified Kočovský carbamylation[8] method to give first **14**, then **15** in 71% and 61% yields, respectively (Scheme 2). Compound **16** was also derived from **12** via treatment with chloroacetylisocyanate (69%). Treatment of **16** using Finkelstein[7] conditions gave iodo product **17** in excellent yield (91%).[9]

Compounds **6a–c**, **9a–c**, **10a–b**, **11a–b**, **12**, and **14–17** were evaluated for antiproliferative activity using murine leukemia L1210, human CD_4^+ T-lymphocyte (CEM), and human cervix

Table 1
Inhibitory effects of the test compounds on the proliferation of murine leukemia cells (L1210), human T-lymphocyte cells (CEM) and human cervix carcinoma cells (HeLa)

Compound	IC_{50}[a] (μg/mL)		
	L1210	CEM	HeLa
3a	3.8 ± 0.3	8.3 ± 2.9	3.2 ± 0.2
6a	>200	>200	>200
6b	106	>200	>200
6c	19 ± 3	125 ± 37	158 ± 60
9a	127 ± 61	⩾200	25 ± 7
9b	56 ± 30	⩾200	72 ± 54
9c	4.1 ± 0.4	11 ± 6	3.0 ± 0.4
10a	0.82 ± 0.48	0.46 ± 0.10	1.6 ± 0.0
10b	6.8 ± 0.1	0.28 ± 0.07	10 ± 1
11a	10 ± 1	77 ± 32	39 ± 1
11b	>100	>100	>100
12	6.7 ± 0.5	7.7 ± 0.7	7.8 ± 1.2
14	5.9 ± 0.5	6.9 ± 0.1	7.5 ± 0.4
15	7.6 ± 0.4	8.3 ± 1.2	5.1 ± 3.9
16	1.9 ± 0.2	1.8 ± 0.2	8.9 ± 1.7
17	7.9 ± 0.6	1.3 ± 0.6	8.4 ± 1.1

[a] 50% inhibitory concentration or compound concentration required to inhibit tumor cell proliferation by 50%.

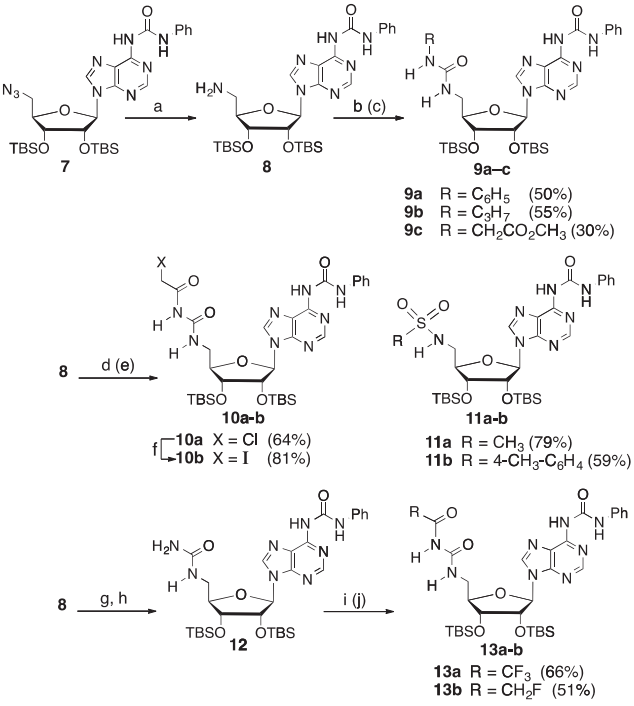

Scheme 1. Reagents: (a) H_2, Pd-C; (b) PhC=N=O; (c) *p*-NO_2-$C_6H_4O_2CNHR$; (d) $ClCH_2CON{=}C{=}O$; (e) RSO_2Cl; (f) NaI; (g) $Cl_3CON{=}C{=}O$; (h) SiOH, MeOH/CH_2Cl_2; (i) CF_3COCl; (j) FCH_2COCl.

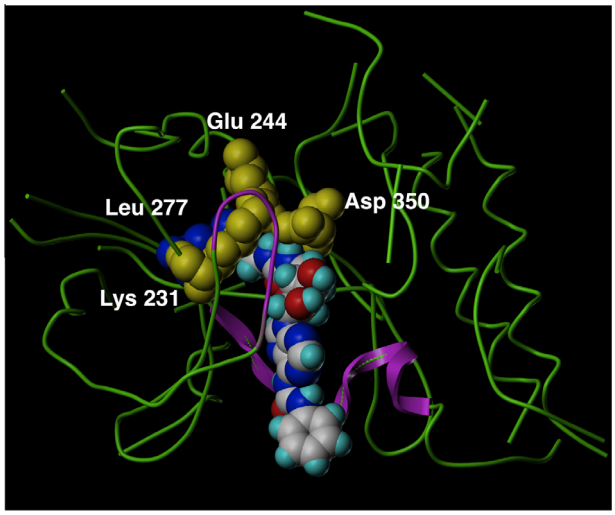

Figure 2. Docking results for **3e** docked into the active site of BMPR1b (pdb 3mdy). Yellow residues: catalytic triad (K231, E244, D350); blue residue: gatekeeper (L277); magenta tube: G-loop or activation loop (I210, G211, K212, G213, R214, Y215, G216); magenta ribbon: hinge region (I278, T279, D280, Y281, H282, E283, N284, G285, S286).